Strap-Down Pedestrian Dead-Reckoning System

Pragun Goyal*, Vinay J. Ribeiro†, Huzur Saran‡ and Anshul Kumar§

Department of Computer Science and Engineering

Indian Institute of Technology Delhi, New Delhi 110016

Email: *pragun.goyal@gmail.com,{†vinay,‡saran,§anshul}@cse.iitd.ac.in

Abstract—This paper presents a waist-worn Pedestrian Dead Reckoning (PDR) System that requires minimal end-user calibration. The PDR system is based on an Inertial Measurement Unit (IMU) comprising of a tri-axial accelerometer, a tri-axial magnetometer and a tri-axial gyroscope. We propose a novel heading estimation scheme using a quaternion-based extended Kalman filter (EKF) that estimates magnetic disturbances and corrects for them. Accelerometer measurements are used to detect step events and to estimate step lengths. Experimental results show that a relative distance error of about 3% to 8% can be obtained using our methods.

Index Terms—Inertial navigation, Dead reckoning

I. Introduction

Indoor environments, street canyons and areas with heavy tree cover are typical examples of places where the GPS fails to perform satisfactorily due to degradation of satellite signals. A popular solution to this problem in the context of Pedestrian Navigation Systems (PNS) is to integrate GPS with an Inertial Measurement Unit (IMU) [1]. Typically, IMU-based Pedestrian Dead Reckoning (PDR) systems model the motion of human body during various activities to overcome the large drift introduced by the numerical integration of IMU measurements [2], [3].

We present a waist-worn IMU based PDRS that requires minimal user-specific calibration (see Figure 1). The IMU contains a tri-axial gyroscope, a tri-axial magnetometer and a tri-axial accelerometer. A waist-worn IMU is more practical for consumer navigation purposes than a shoe-mounted one which requires an IMU to be attached to the shoe [4], [5], [6], [7], [8], [9]. Typically, systems using foot mounted IMUs benefit from Zero-Velocity Updates, that can be performed during the stance phase, as the foot is stationary. However, waist-worn systems need more sophisticated algorithms for navigation because the pelvis does not have similar zero-velocity points during walking motion. The techniques described in this paper can be extended to placement of the IMU on those parts of body that move with the pelvis. This includes the case where the device is carried in a trouser pocket [10].

We propose the use of a quaternion based extended Kalman filter (EKF) to estimate the full 3D attitude of the sensor module. A full 3D estimation of the attitude allows correction of sensor measurements for changes in tilt of the IMU. Simple numerical integration of the gyroscope data introduces drift
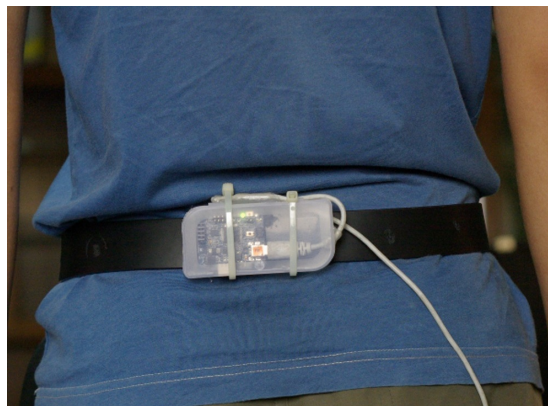
Fig. 1. Sensor module worn by a user

errors and is insufficient for heading estimation. Some of these errors can be reduced by combining the gyroscope data with magnetometer data. However, magnetic disturbances introduce errors in the heading obtained from magnetometers. Our method allows estimation of the magnetic disturbance thereby increasing estimation accuracy.

We use the method described by Wienberg et al. to perform step length estimation [11]. This method is known to perform well even if generalized calibration values are used for different users [10]. Various other kinetic models have been proposed to estimate the step length using accelerometer measurements [12], [13], [14], [11]. These models, however, require that some parameters be tuned for every different user. Although user specific calibration typically results in more accurate estimation of step length, acquiring data for calibration is quite challenging. This is especially true for kinetic models that are sensitive to external factors like hardness of floor, footwear, etc., as user specific parameters need to be re-tuned for these changes.

Several methods have been proposed to compute user specific parameters for different kinetic models using GPS data [15]. These methods automate the collection of user specific training data and the computation of user parameters. However, as it takes some time to collect training data, a minimal calibration system, such as ours, can be used to estimate the position while training data is collected. It can also prove useful in situations where user specific calibration can not be done due to the lack of GPS and Indoor Map data.

II. HEADING ESTIMATION

Gyroscopes and magnetometers are popularly used in dead reckoning systems to estimate the heading. Gyroscope measurements contain bias and scale errors which introduce a drift in the heading estimate. A well calibrated compass, on the other hand, is known to give a stable heading. However, external magnetic disturbance due to electronic systems, power lines, magnetic objects like speakers, motors are known to degrade the performance of a compass. This is especially true for indoor environments.

Among various techniques proposed to counter the errors introduced by magnetic disturbance, Gusenbauer et al. have described a method that uses a simple linear recursive filter to estimate the heading using only magnetometer measurements [15]. This method uses a filter weight parameter that can take different values for different users. Besides, as the experimental setup described by Gusenbauer et al. does not include a gyroscope, the compass tilt-compensation has to be performed using only accelerometer data.

As a three-axis gyroscope is fast becoming a standard feature in smartphones and Personal Digital Assistant (PDA) devices, more sophisticated techniques can be used to counter the errors introduced by indoor magnetic disturbance. Moreover, as the rotation of IMU is not constrained to the vertical axis, a full 3D attitude estimation can achieve better heading accuracy by incorporating gyroscope measurements for three orthogonal axes.

We propose that an EKF be used to estimate the full 3D attitude of the IMU using the data from the gyroscope, the magnetometer and the accelerometer. Owing to several computational benefits offered by quaternions over other attitude representations including Euler angles and Direction Cosine Matrix (DCM) [16], we chose to represent the full 3D attitude as a quaternion.

A. Quaternion Mathematics

For the sake of completeness, we shall provide a brief mathematical description of quaternions. Quaternions extend the complex number system and can be expressed as,

$$q = q_0 + q_1 i + q_2 j + q_3 k. \tag{1}$$

The 3-D orientation of an object expressed as a quaternion offers several advantages over Euler angles or DCMs. In the following equations, the attitude of the body with respect to ground is given by the quaternion q [17]. A 3×1 vector $(\vec{x})$ can be transformed from its representation in a reference frame (N) fixed on the ground $(\vec{x}^N)$ to its representation in a reference frame (B) fixed on the object $(\vec{x}^B)$, using,

$$\vec{x}^B = C_N^B(q)\vec{x}^N, \tag{2}$$

where $C_N^B(q)$ is the 3-D rotation matrix obtained from the quaternion (q) as follows,

$C_N^B(q) =$
$$\begin{bmatrix} (q_0^2 + q_1^2 - q_2^2 - q_3^2) & 2(q_1q_2 + q_0q_3) & 2(q_1q_3 - q_0q_2) \\ 2(q_0q_3 + q_1q_2) & (q_0^2 - q_1^2 + q_2^2 - q_3^2) & 2(q_2q_3 - q_0q_1) \\ 2(q_1q_3 - q_0q_2) & 2(q_0q_1 + q_2q_3) & (q_0^2 - q_1^2 + q_2^2 + q_3^2) \end{bmatrix}$$

The reverse transformation matrix (C_B^N) can be simply obtained as the transpose of (C_N^B).

A quaternion $(q = q_0 + q_1 i + q_2 j + q_3 k)$ can be rotated by multiplying it with a quaternion representing the spatial rotation $(r = r_0 + r_1 i + r_2 j + r_3 k)$. The resulting quaternion $(q' = q_0' + q_1' i + q_2' j + q_3' k)$ can be obtained as,

$$q' = \begin{bmatrix} q_0' \\ q_1' \\ q_2' \\ q_3' \end{bmatrix} = q \otimes r = \begin{bmatrix} q_0 r_0 - q_1 r_1 - q_2 r_2 - q_3 r_3 \\ q_1 r_0 + q_0 r_1 - q_3 r_2 + q_2 r_3 \\ q_2 r_0 + q_3 r_1 + q_0 r_2 - q_1 r_3 \\ q_3 r_0 - q_2 r_1 + q_1 r_2 - q_0 r_3 \end{bmatrix} \tag{3}$$

B. Magnetic Disturbance

We estimate the magnetic disturbance using the EKF. Our method involves estimation of magnetic disturbance in a reference frame fixed with respect to ground, as the magnetic disturbance is a property of a particular location. This is different from several other techniques proposed to handle the errors introduced by magnetic disturbances. Sabatini et al. have described a quaternion based EKF in which, the magnetic disturbance is estimated as magnetometer bias error in the state vector [18]. This is equivalent to estimation of a magnetic disturbance vector fixed with respect to the sensor module. Among other techniques, Roetenberg et al. employ a Complementary Filter (in contrast to the EKF of our method) that models the errors introduced by magnetic disturbance [19].

A magnetometer measures the total magnetic field $(\vec{H})$ at a point, which is given by,

$$\vec{H} = \vec{H}_{earth} + \vec{H}_{ext} \tag{4}$$

where $\vec{H}_{earth}$ and $\vec{H}_{ext}$ denote the Earth's magnetic field at the point and the external magnetic field respectively.

$\vec{H}_{ext}$ can be split into two components, $\vec{d}$ and $\vec{H}_{sys}$, where $\vec{H}_{sys}$ is the constant magnetic field generated by the navigation system (including the user) and $\vec{d}$ is the magnetic disturbance generated by surroundings,

$$\vec{H}_{ext} = \vec{H}_{sys} + \vec{d}. \tag{5}$$

It is assumed that the contribution of $\vec{H}_{sys}$ is removed from the raw measurement during sensor calibration. As $\vec{d}$ cannot be measured directly, it has to be estimated indirectly.

C. Extended Kalman Filter

We will now describe the EKF. The state vector (x) for the filter is composed of the rotation quaternion $(q = [q_1, q_2, q_3, q_4])$, augmented by the tri-axial gyroscope scale $(s = [s_x, s_y, s_z])$ and bias factors $(\vec{b} = [b_x, b_y, b_z])$ and external magnetic disturbance vector $(\vec{d}^N = [d_x, d_y, d_z])$, that is,

$$x = [q, s, \vec{b}, \vec{d}].\tag{6}$$

A Kalman Filter typically involves alternating state prediction and state update phases. These phases are detailed below.

State Prediction Step:

The state prediction step in a Kalman Filter involves projecting the filter state vector for the next measurement,

$$\bar{x}_t = f(x_{t-1}, u_t) + w_t \tag{7}$$

where $\bar{x}_t$ is the projected state vector, x_{t-1} is the initial state vector, u_t is the control input, f is the process model and w_t represents Gaussian process noise.

The state covariance (P_{t-1}) is projected using,

$$\bar{P}_t = F_t P_{t-1} F_t^T + Q_t,\tag{8}$$

where $\bar{P}_t$ is the projected covariance, F_t is the linearized process model, obtained as the Jacobian of the process model (f), and Q_t is the process noise.

In our implementation, the control input u_t is obtained from gyroscope inputs. As described in [16], for the discrete case the gyroscope readings can be incorporated in the attitude quaternion (q_t) by multiplying it by a quaternion (r_t) representing the change in orientation during the sampling period ΔT, given by,

$$\bar{q}_t = q_{t-1} \otimes r_t + {}^q w_t,\tag{9}$$

where $\otimes$ represents quaternion multiplication (equation 3) and ${}^q w_t$ represents Gaussian noise. r_t is obtained from the gyroscope readings after correcting for scale and bias errors as follows.

$$r_t = \begin{bmatrix} a_{t,c} \\ a_{t,s}\sigma_{t,x} \\ a_{t,s}\sigma_{t,y} \\ a_{t,s}\sigma_{t,z} \end{bmatrix}\tag{10}$$

where

$$\sigma_t = \begin{bmatrix} \sigma_{t,x} \\ \sigma_{t,y} \\ \sigma_{t,z} \end{bmatrix} = \begin{bmatrix} (s_{t,x}\omega_{t,x} - {}^g b_{t,x})\Delta T \\ (s_{t,y}\omega_{t,y} - {}^g b_{t,y})\Delta T \\ (s_{t,z}\omega_{t,z} - {}^g b_{t,z})\Delta T \end{bmatrix} + {}^g w_t,\tag{11}$$

$[\omega_{t,x}, \omega_{t,y}, \omega_{t,z}]$ denotes the raw measurements of the gyroscope along x, y and z axes, ${}^g b_{t,x}$, ${}^g b_{t,y}$ and ${}^{b_{t,z}}$ are gyroscope bias terms and ${}^g w_t$ is Gaussian noise. The values of $a_{t,c}$ and $a_{t,s}$ depend on the chosen order of approximation of quaternion integration [16]. We found that the first order approximation with $a_{t,c} = 1$ and $a_{t,s} = 1/2$ performs satisfactorily for a PDRS.

The scale and bias corrections for the gyroscope, and the external magnetic disturbance vector are modeled as a random walk, given by,

$$\bar{s}_t = s_{t-1} + {}^s w_t,\tag{12}$$

$$\bar{b}_t = b_{t-1} + {}^b w_t,\tag{13}$$

$$\bar{\vec{d}}_t = \vec{d}_{t-1} + {}^d w_t,\tag{14}$$

where ${}^s w_t, {}^b w_t, {}^d w_t$ are 1×3 vectors representing Gaussian noise terms.

Measurement Update Step:

The measurement update step of a Kalman Filter involves refining the state estimate by incorporating sensor measurements. The update step requires the computation of the Jacobian (H_t) (see footnote 1) of the measurement model (h),

$$\bar{z}_t = h(\bar{x}_t) + v_t,\tag{15}$$

where z_t is the estimated sensor measurement at the kth interval and v_t represents Gaussian sensor noise.

The Kalman gain (K_t) is computed as,

$$K_t = \bar{P}_t H_t^T (H_t \bar{P}_t H_t^T + V_t)^{-1},\tag{16}$$

where, $\bar{P}_t$ is the projected covariance from the last state prediction step and V_t represents Gaussian noise. The state vector is updated as,

$$x_t = \bar{x}_t + K_t(z_t - h(\bar{x}_t)),\tag{17}$$

where x_t is the updated state vector, $\bar{x}_t$ is the predicted state vector from the last state prediction step and z_t are sensor measurements. The covariance matrix is updated as,

$$P_t = (I - K_t H_t)\bar{P}_t,\tag{18}$$

where P_t is the updated state covariance and I is the identity matrix. [1]

We shall now describe our measurement model. We assume the accelerometer and magnetometer measurement noise to be uncorrelated zero mean white noises. Independent update steps are performed for the magnetometer and accelerometer readings.

The magnetometer measurement (${}^m \vec{z}_t$) can be modeled as,

$${}^m \vec{z}_t = C_N^B(q_t)(\vec{H}_{earth}^N + \vec{d}_t^N) + {}^m \vec{v}_t,\tag{19}$$

where $C_B^N(\bar{q}_t)$ is the reference frame transformation matrix derived from $\bar{q}_t$, $\vec{H}_{earth}^N$ is the magnetic field due to Earth in the ground reference frame, d_t^N is the estimated magnetic disturbance and ${}^m \vec{v}_t$ represents Gaussian noise.

Besides the gyroscope and magnetometer, the accelerometer also provides information about the attitude of the IMU. This is due to the fact that gravity always acts along the vertical axis. However, the accelerometer measurement is used to perform an update step only if the variance of accelerometer signal, computed over a running window of length 1 second is below a fixed threshold. It is assumed that if the accelerometer signal remains constant for a long time, then the user is at rest. Hence, acceleration measured by the accelerometer ($\vec{a}$) can be assumed to be equal to gravity ($\vec{g}$). The accelerometer measurement in this condition (${}^a \vec{z}_{k+1}$) can be modeled as,

$${}^a \vec{z}_t = C_N^B(q_t)(\vec{g}^N) + {}^a \vec{v}_t,\tag{20}$$

where $\vec{g}^N$ is the gravity vector in ground reference frame and ${}^a \vec{v}_t$ represents Gaussian noise.

---

[1]Please note that H_t used in equations 16, 17 and 18 represents the Jacobian of the measurement model where as H used elsewhere in this paper represents magnetic field.
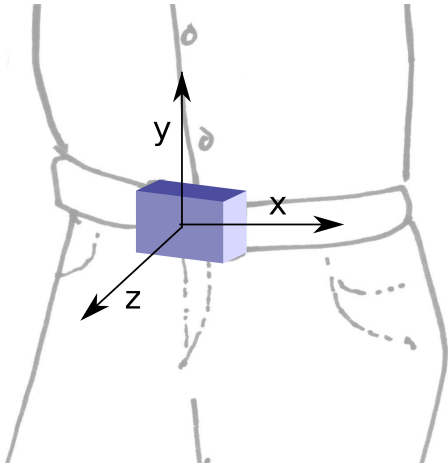
Fig. 2.   Sensor module reference frame

D. Heading from 3D attitude

The EKF estimates the 3D attitude of the sensor module. We compute the heading as the angle between anterior-posterior vertical plane and a vertical reference plane fixed with respect to ground. This method assumes that the IMU stays fixed on the user.

In order to compute this angle, we take a vector $\vec{u_t}^B$ fixed on the sensor module, such that it is not collinear with the vertical axis of the ground reference frame. The representation of this vector in the ground reference frame $\vec{u_t}^N$ can be obtained using the following equation.

$$\vec{u_t}^N = C_B^N(q_t)\vec{u_t}^B \tag{21}$$

The horizontal projection $\vec{u_t}^{N,horz}$ of this vector can be obtained simply by,

$$\vec{u_t}^{N,horz} = \begin{bmatrix} 1 & 0 & 0 \\ 0 & 1 & 0 \\ 0 & 0 & 0 \end{bmatrix} \vec{u_t^N} \tag{22}$$

Heading (θ_t) is obtained as the angle that $\vec{u_t}^{N,horz}$ makes with either of the horizontal axes fixed on ground. In our implementation, we choose $\vec{u_t}^B$ as a unit-vector along the z-axis of the reference frame fixed on the sensor (Figure 2) module.

III. STEP DETECTION AND STEP LENGTH ESTIMATION

In this section we will describe the step detection and step length estimation techniques used to estimate the distance moved by the user.

A. Step Event Detection

Our step event detection scheme is based on the description of waist accelerometry given by Zijlstra et al. [20], [14]. It relies on the fact that each step even involves the rise and fall of the pelvis. We estimate the vertical displacement of the pelvis by double integrating the vertical acceleration. The vertical displacement thus obtained, however, has a large integration drift. In order to remove this drift, it is filtered

using a zero-lag high-pass Butterworth filter with a cut-off frequency of 0.1 Hz [20].

Steps are detected as peaks in the resulting vertical displacement (Figure 3). As the numerical integration itself acts as a low-pass filter, the resulting curve is smooth and no further low pass filtering is required. However, there are some extraneous peaks for each step. To get rid of these extra peaks, we ensure that only one step occurrence is detected for each zero crossing of the vertical displacement.

Each step event begins with an Initial Contact (IC) (Figure 4), after which the body swings forward on a single foot. This is followed by the Final Contact (FC), which marks the beginning of the double stance phase, during which both feet remain on the ground. Our step length estimation (section III-B) technique requires that ICs be detected for each step. Once a step event is detected, the Initial Contact (IC) for the step is detected as the highest local maximum in the anterior-posterior acceleration between the peak in the vertical displacement corresponding to the previous step and the peak in the vertical displacement corresponding to the next step.
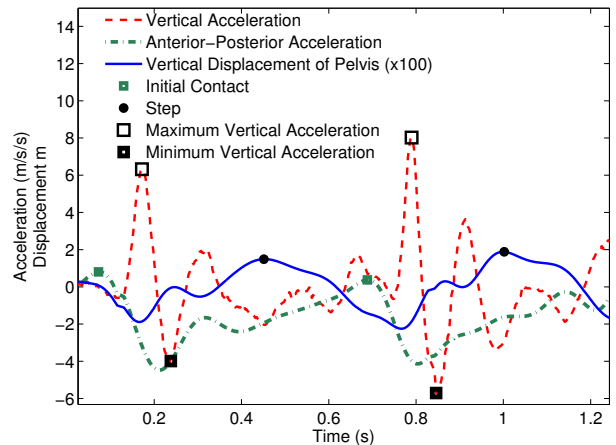

Fig. 3.   Step Detection using accelerometer data. The vertical displacement is multiplied by 100 to make it comparable to vertical and anterior-posterior acceleration.

B. Step Length Estimation

Several step length estimation techniques have been devised for different applications. Levi and Judd have described a technique in which step length is modeled as a linear function of step frequency [12]. Jeong et al. have described a method that does not need to be calibrated for different users. However, their method assumes that the IMU is worn near the foot [13]. Zijlstra et al. have described an inverted pendulum model for the motion of pelvis during a step [14]. This method requires the leg length to be measured experimentally and is known to be sensitive to user calibration [10]. Wienberg et al. [11] have proposed an approximation of the popular inverted pendulum model described by Zijlstra et al. [14], [20], that does not require knowledge of the leg length. In prior work, a comparison of several popular step length estimation schemes
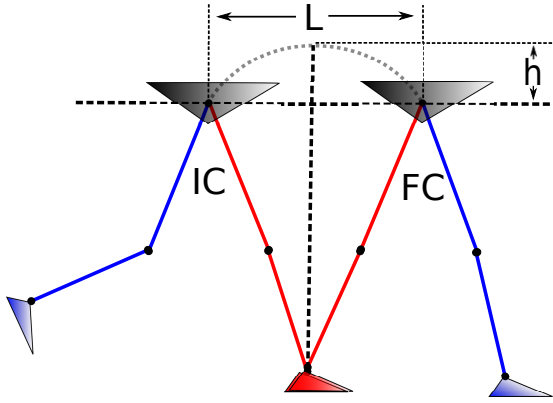
Fig. 4. Motion of the pelvis during a step

Volunteer S.No	Maximum Relative distance error over the entire path	Average Relative distance error
1	5.31%	3.48%
2	8.84%	5.66%
3	5.14%	3.65%
4	5.53%	3.62%
5	7.65%	4.69%
6	8.15%	5.75%
7	8.38%	5.14%
8	4.23%	3.58%
9	18.44%	7.99%

has revealed that the technique described by Wienberg et al. [11] is best suited for a waist mounted IMU using generalized calibration values [10].

The method proposed by Wienberg et al., estimates the length of the step (L) (Figure 4) from the vertical displacement of the pelvis (h). They have empirically demonstrated that the step length can be approximated as [11],

$$L = K \sqrt[4]{a_{max} - a_{min}}, \tag{23}$$

where a_{max} and a_{min} denote the maximum and minimum vertical acceleration during a step respectively and K is a multiplication factor. The value of K is different for different people, and can be found out experimentally. We compute the values for a_{max} and a_{min} from the IC of each step to the IC of succeeding step.

IV. INDOOR EXPERIMENTS AND RESULTS

We used the iNemo IMU module developed by ST Microelectronics to collect data. The module is mounted on an adjustable waist belt (Figure 1 and 2). The module samples sensor data for a tri-axial accelerometer, a tri-axial gyroscope and a tri-axial magnetometer at 50Hz and transfers the raw data to a laptop over USB, which in turn timestamps and logs it. The collected data is processed offline using MATLAB.

Experiments were preformed at two different indoor locations to collect walk data for different users. The first set of experiments were performed in a corridor on the first floor of Old O.T Block, All India Institute of Medical Sciences (AIIMS). Data was collected for 9 volunteers at this location. We also collected data for 6 volunteers in a second set of experiments performed in a corridor on the third floor of Bharti School of Telecommunication and Management at India Institute of Technology (IIT) Delhi.

In order to establish the ground truth trajectory, the subjects were made to walk on a manually surveyed path marked on the corridor floor. In both experiments the path starts and ends at the same position. Both paths had several straight stretches followed by sharp right-angle turns in clockwise and anti-clockwise directions to test the accuracy of our attitude estimation scheme.

We use a measure of relative distance error to evaluate the accuracy of our method. For any point in the estimated trajectory, the relative distance error is the ratio of the distance between the estimated position and the actual ground truth position, and the length of the path up to that point from the starting position. We evaluate this relative distance error for the final position as well as all other sharp turns in trajectories. Average values for relative error presented below correspond to the average of relative error at all these points corresponding to sharp turns.

The value of the scaling term (K) described in equation (23) was computed for different subjects by making them walk on a straight path of the known length. We chose the mean of this distribution, as the generalized value of K. This value came out to be 0.49. The same value of K was used to generate trajectories for all subjects.
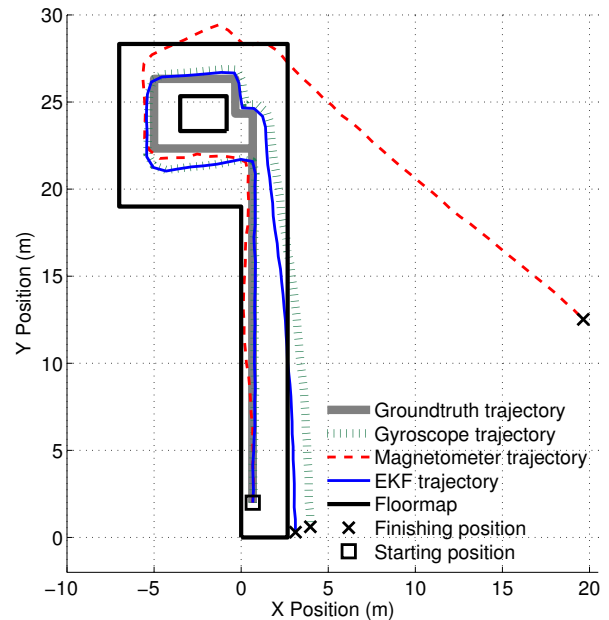

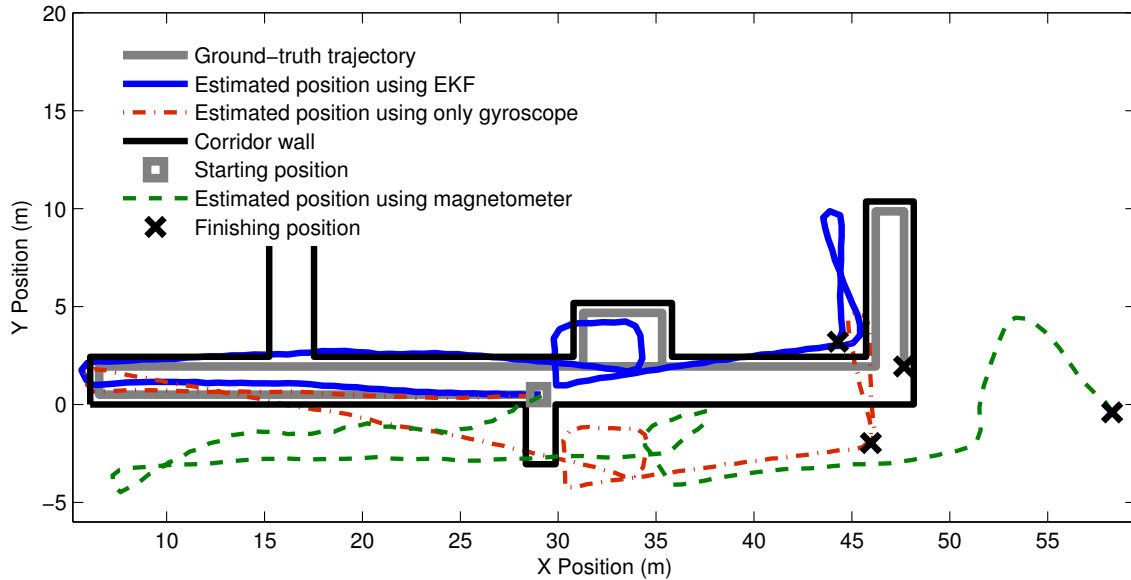Fig. 5. Indoor Results: AIIMS
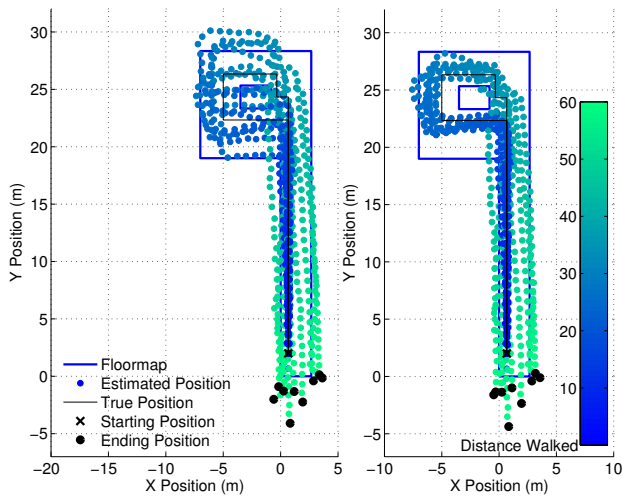
Fig. 7.   Indoor Results: IIT Delhi

Fig. 6.   Degradation of estimation accuracy with distance travelled. Left: Estimated positions for all volunteers using K=0.49. Right: Estimated position of all volunteers for K such that the average error for the path is minimum.

A. Results: AIIMS

Figure 5 shows one of the results obtained for a experiment performed at AIIMS. The figure shows three estimated trajectories obtained by using only the gyroscope, only the magnetometer and the EKF filter. These trajectories are discussed in detail in sections IV-B1, IV-B2 and IV-B3. The value of the scaling term described in equation (23) was again taken to be 0.49. The maximum relative distance error over the entire path was obtained to be 5.53%. As is evident from the figure, the estimated position obtained using only the magnetometer has

a large error. The total length of the path is 59.0m.

Figure 6 shows the estimated trajectories for all the 9 volunteers overlaid on the same plot. Table I captures the average and maximum relative distance errors observed for different subjects in this experiment. The average error varied from 3.48% to 8% and the worst case relative distance error varied between 4.23% and 18.44%. Note that these errors were obtained for the case with $K = 0.49$ for all volunteers, that is the minimal calibration scenario. If we chose K suitably for each user, as can be seen in the right half of Figure 6, a significant increase in accuracy is possible. The worst case relative distance error obtained in this case improved to 9%.

B. Results: IIT Delhi

Figure 7 shows the results obtained for an exemplary experiment performed at IIT Delhi. The figure shows three estimated trajectories obtained by using only the gyroscope, only the magnetometer and the EKF filter. The total distance walked in the experiment in a total of 159 steps was 94.37m. The duration of the experiment was 88.6 seconds. We shall now compare the three different trajectories. The results obtained in this set of experiments were similar to the results obtained in the experiments performed at AIIMS (Section IV-A).

1) Only Gyroscope: User position was estimated using the proposed EKF but with no updates performed for magnetometer measurements. It must, however, be noted that the accelerometer updates were performed as described in Section II-C. As expected, when the heading is estimated using only the gyroscope measurements, the heading estimate starts drifting. The total error observed in the estimated position at the end of the experiment is 4.26m which translates to a 4.51% relative distance error.

2) Only Magnetometer: User position was estimated using only the magnetometer. The total error observed in the estimated position at the end of the experiment is 10.89m which translates to a 11.53% relative distance error.

3) Extended Kalman Filter using both Gyroscope and Magnetometer: The total error observed in the estimated position at the end of the experiment is 3.61m which translates to a 4% relative distance error. Although the relative distance error for this case is very similar to the case where only the gyroscope is used to estimate the heading, it can be seen in the figure that the average error in the estimated position, when measured over the entire path is much worse for the latter.

V. CONCLUSIONS AND FUTURE WORK

We have presented a waist worn IMU based PDRS that requires minimal calibration on the user end. The obtained average relative distance error of 3 to 8%, is encouraging and comparable to other handheld systems [15] and foot mounted systems [6].

The techniques and results discussed so far have been in the context of a waist worn system, however, it is possible to extend these to other placements of the IMU. The step length estimation technique described is known to work for the case where in the IMU is carried in a trouser pocket [10]. Besides, a full 3D estimation of the attitude allows for an estimation of heading in cases where the IMU changes its 3D orientation. However, our heading estimation technique assumes that the IMU is fixed on the user's body. Given the flat shape of most PDAs and cellphones, this assumption would hold for most of the time when the device is carried in a trouser pocket as long as it does not move or flip inside the pocket. Modeling the changes in the relative orientation of the IMU with respect to the user as a solution to these challenges represents a possible direction for future work.

VI. ACKNOWLEDGEMENTS

REFERENCES

[1] C. M. Godha S., Lachapelle G., "Integrated GPS/INS system for Pedestrian Navigation in a Signal Degraded Environment," *Proceedings of the 19th International Technical Meeting of the Satellite Division of The Institute of Navigation (ION GNSS 2006)*, pp. 2151–2164, September 2006.

[2] Y. K. Thong, M. S. Woolfson, J. A. Crowe, B. R. Hayes-Gill, and D. A. Jones, "Numerical double integration of acceleration measurements in noise," *Measurement*, vol. 36, no. 1, pp. 73 – 92, 2004.

[3] Y. K. Thong, M. S. Woolfson, J. A. Crowe, B. R. Hayes-Gill, and R. E. Challis, "Dependence of inertial measurements of distance on accelerometer noise," *Measurement Science and Technology*, vol. 13, no. 8, p. 1163, 2002.

[4] S. Godha and G. Lachapelle, "Foot mounted inertial system for pedestrian navigation," *Measurement Science and Technology*, vol. 19, no. 7, p. 075202, 2008.

[5] S. Y. Cho and C. G. Park, "MEMS Based Pedestrian Navigation System," *The Journal of Navigation*, vol. 59, no. 01, pp. 135–153, 2006.

[6] R. Feliz, E. Zalama, and J. Gomez, "Pedestrian tracking using inertial sensors." Red de Agentes Fsicos, 2009.

[7] A. Jimenez, F. Seco, C. Prieto, and J. Guevara, "A comparison of Pedestrian Dead-Reckoning algorithms using a low-cost MEMS IMU," Aug. 2009, pp. 37 –42.

[8] S. Beauregard, "Omnidirectional Pedestrian Navigation for First Responders," *Positioning, Navigation and Communication, 2007. WPNC '07.*, pp. 33 –36, Mar. 2007.

[9] N. Castaneda and S. Lamy-Perbal, "An improved shoe-mounted inertial navigation system," in *Indoor Positioning and Indoor Navigation (IPIN), 2010 International Conference on*, 2010, pp. 1 –6.

[10] J. Jahn, U. Batzer, J. Seitz, L. Patino-Studencka, and J. Gutie andrrez Boronat, "Comparison and evaluation of acceleration based step length estimators for handheld devices," in *Indoor Positioning and Indoor Navigation (IPIN), 2010 International Conference on*, 2010, pp. 1 –6.

[11] H. Wienberg, "Using the ADXL202 in Pedometer and Personal Navigation Applications," *Analog Devices AN-602 application note*, 2002.

[12] J. T. Levi, Robert W., "Dead reckoning navigational system using accelerometer to measure foot impacts," Patent 5 583 776, December, 1996.

[13] Kim J.W, Jang H., Hwang D-H, and Park C., "A step, stride and heading determination for the Pedestrian Navigation System," *Journal of Global Positioning Systems, vol. 3*, pp. 273–279.

[14] W. Zijlstra and A. L. Hof, "Displacement of the pelvis during human walking: experimental data and model predictions," *Gait & Posture*, vol. 6, no. 3, pp. 249 – 262, 1997.

[15] D. Gusenbauer, C. Isert, and J. Kro andsche, "Self-contained indoor positioning on off-the-shelf mobile devices," in *Indoor Positioning and Indoor Navigation (IPIN), 2010 International Conference on*, 2010, pp. 1 –9.

[16] D. Titterton and J. Weston, *Strapdown Inertial Navigation Technology*, 2nd ed. The American Institute of Aeronautics and Astronautics, 2004.

[17] J. B. Kuipers, "Quaternions and rotation sequences," *Proceedings of the First International Conference on Geometry, Integrability and Quantization*, Sep 1999.

[18] A. M. Sabatini, "Quaternion-based extended Kalman filter for determining orientation by inertial and magnetic sensing," *IEEE Transactions on Biomedical Engineering*, vol. 53, no. 7, pp. 1346–1356, 2006.

[19] D. Roetenberg, H. Luinge, and P. Veltink, "Inertial and magnetic sensing of human movement near ferromagnetic materials," in *ISMAR '03: Proceedings of the 2nd IEEE/ACM International Symposium on Mixed and Augmented Reality*. Washington, DC, USA: IEEE Computer Society, 2003, pp. 268–269.

[20] W. Zijlstra, "Assessment of spatio-temporal parameters during unconstrained walking," *European Journal of Applied Physiology*, vol. 92, pp. 39 – 44, 2004.